Dielectric properties of *Pouteria sapota* compounds in terahertz frequency range

H. Vilchis
Instituto de Investigación e Innovación en Energías Renovables, Universidad de Ciencias y Artes de Chiapas, Libramiento Norte 1150, Tuxtla Gutiérrez, Chiapas, 29039, México.

M. F. López-Páez
Instituto de Investigación e Innovación en Energías Renovables, Universidad de Ciencias y Artes de Chiapas, Libramiento Norte 1150, Tuxtla Gutiérrez, Chiapas, 29039, México.

J. Conde
Cátedra - Conahcyt, Instituto de Investigación e Innovación en Energías Renovables, Universidad de Ciencias y Artes de Chiapas, Libramiento Norte 1150, Tuxtla Gutiérrez, Chiapas, 29039, México.

E. Briones
Departamento de Matemáticas y Física, Instituto Tecnológico y de Estudios Superiores de Occidente, Universidad Jesuita de Guadalajara, Tlaquepaque, 45604 Jalisco, México.

G. López-Morales
Instituto de Investigación e Innovación en Energías Renovables, Universidad de Ciencias y Artes de Chiapas, Libramiento Norte 1150, Tuxtla Gutiérrez, Chiapas, 29039, México.

Received 19 December 2023; accepted 24 April 2024

The analysis and the mathematical approximation of the dielectric properties of *Pouteria sapota* (Mamey) pulp compounds in the Terahertz (THz) range are presented. Since THz electromagnetic waves show a high sensitivity to detect water content when interacting with organic materials, this technique was used to determine the effective dielectric function (EDF) of four samples with different water contents from the THz spectrum data. By fitting the EDF to the Landau-Lifshitz-Looyenga (LLL) dielectric mixture equation, the theoretical dielectric functions of each pulp compounds were approximated. The approach proposed here not only considered dry matter and water content in the *Pouteria sapota* pulp, as has been reported in the literature for organic samples, but also included the contribution of the volatile components (VC) that allowed a better adjustment to the experimental results. The water and VC content increase the value of the real and imaginary part of the calculated EDF in the wet samples. The use of the non-destructive THz spectroscopy technique allows determining the dielectric properties of fruits that have been dehydrated. Therefore, the methodology proposed here can be used as a method of in situ and ex situ quality control in the agri-food industry.

Keywords: Effective dielectric function; terahertz frequency; dielectric properties; pouteria sapota.

DOI: https://doi.org/10.31349/RevMexFis.70.051303

1. Introduction

Monitoring quality of dehydration of agricultural products, as well as the conservation of their nutrients during this process is of importance for the food industry. There are several perishable and seasonal fruits or vegetables rich in vitamins, mineral salts, antioxidants, and fiber that are beneficial to human health, and its preservation for later consumption is of interest. One of them is *Pouteria sapota*, a tropical fruit native to Central America and particularly southern Mexico, which is characterized for being beneficial to health due to its high content of carotenoids [1-3]. In addition, this fruit is mostly composed of 63.8 % of water, the rest being fiber content, carbohydrates, minerals and vitamins A and C. Hence, it is essential that the food industry not only use conservation techniques to take advantage of the nutritional properties of agricultural products, but also develops methods for the rapid assessment of the quality and safety of the product during the dehydration process.

Food drying is a preservation method that consists of extracting water from the product through the circulation of hot air with the aim of inhibiting the growth of bacteria, yeasts, and mold inside [4]. During the dehydration process, the loss of some volatile organic compounds, such as temperature-sensitive vitamins, corresponding to the flavor and aroma of the food may also occur [5]. Up to 21 compounds have been identified for the pulp of *Pouteria sapota*, among which are mainly terpenoids and esters, followed by aromatic hydrocarbons, aldehydes, alcohols, and ketones [6]. Therefore, it is of interest to develop a drying quality monitoring system that verifies the water content and the concentration of its nutrients until the complete drying of the product. There are optical non-invasive techniques able to detect the moisture content and the chemical composition of food. A recent publication evidences the use of spectroscopic techniques to

study the water content and the presence of carotenoids in *Pouteria sapota* pulp [7]. Infrared technology allows detection of moisture content, but they are limited by the poor resolution and the strong absorption of water molecules in this region [8,9]. On the other hand, Terahertz time-domain spectroscopy (THz-TDS) is a non-destructive technology useful for examining food quality with higher resolution and sensitivity at molecular vibration, and its radiation does not ionize or damage an organic sample [10-12]. Electromagnetic waves in the range from 0.1 THz to 30 THz show a high sensitivity to the presence of water molecules in food; this interaction causes a change in the amplitude and phase of the transmitted reference signal depending on the water content in an organic sample [13-15]. The analysis of these variations allows to indirectly determine the optical properties such as the complex refractive index and the absorption coefficient, as well as the dielectric function of the sample. These parameters are useful for theoretically modeling fruit constituents and understanding their interaction with the THz electromagnetic waves [11,16,17]. In addition to the fact that this technique has applications in food inspection, it also has them in the pharmaceutical and medical industry, including in the communication, remote sensing, and astronomy area [18]. Several works have studied the dielectric properties of food in the Megahertz, Gigahertz and microwaves range, varying factors as their composition, temperature, frequency range, and moisture content [19-21]. In the last decade, the THz spectroscopy has revealed its usefulness in the detection of protein and amino acids in dried foods [12,22]. Likewise, it can be applied to quantitatively detect the water content in dried samples and other types of foods [10-14,23]. Some studies have proven that the dielectric function can be modified depending on the composition of the food [20,24]. For instance, Shiraga et al. investigated the content of monosaccharides (glucose and fructose) and disaccharides (sucrose and trehalose) based on the analysis of their dielectric response in the THZ range [25,26]. Since fruits are characterized by having sugars and other volatile compounds, this technique is optimal for the analysis of their nutritional content.

In this work, THz-TDS is performed to determine the experimental effective dielectric function of the *Pouteria sapota* pulp samples with different water contents: 0%, 15.53%, 20.16% and 40.59%. In the approximation of the EDF, some authors consider an organic sample composed only of dry matter and water [27,28]. However, we propose to include in the theoretical adjustment the contribution of some volatile components, which represent important components that affect the organoleptic properties of food. Through the analysis of the calculated EDF, it is possible to determine the dielectric function and the volumetric fraction of water, dry matter, and the VC contained in the pulp of this fruit, applying an effective medium theory model, such as the Landau-Lifshitz-Looyenga dielectric mixture equation. The proposed methodology can be applied to know the dielectric function of any other organic product that undergoes a dehydration process.

2. Dehydration process of *Pouteria sapota* and THz system description

Pouteria sapota was obtained in a local market in Tuxtla Gutiérrez, Chiapas, México. The ripening, texture, color, and physical effects, such as bumps or fungi presence, were considered for the selection of the fruit [3,7]. The fruit was carefully cleaned and washed with soap and water, removing microorganisms and solid particles on the outside of the peel. The shell and seed were then removed. Using a kitchen slicer, four slices of this fruit with an area of 50×30 mm and a thickness of 1.59 ± 0.18 mm were obtained. Since a fresh sample has a high water content that can cause almost complete attenuation of the THz signal, it was decided to consider samples with a water content less than 45%. Therefore, the slices were dehydrated under controlled laboratory conditions using an electric drying chamber (Binder Mod.ED56) at 50 °C. The drying time depended on the desired water content in the sample. The quantification of the water content in the *Pouteria sapota* samples was by means of the gravimetric method [7], which consisted of registered the weight of the sample during a certain drying time by using an analytical balance (Pioneer PX, OHAUS) with a resolution of 0.01 mg. The water content percentage ($WC\%$) on a wet basis was calculated through Eq. (1), where W_t is the current weight in time t and W_d is the dry mass of sample.

$$WC(\%) = \frac{W_t - W_d}{W_t} \times 100\%. \tag{1}$$

The dehydration time of the samples were 90 min, 100 min, 295 min and 525 min to achieve a WC of 40.59%, 20.16%, 15.53% and 0%, respectively. Note that the dry sample has a $WC = 0\%$. The thickness for the sample with the highest water content was 0.92 mm and for the dry sample it was 0.61 mm.

After of the drying process, the time-domain THz transmission spectra of the four samples with different water contents were measured by Picometrix spectrometry (Picometrix T-Gauge, Model T-Ray 5000) in transmission geometry. It was also necessary to obtain the reference spectrum that corresponds to air. THz-TDS system was configured so that data was acquired with a 0.1 ps resolution and each measurement was an average of 1000 scans/second. To evaluate the repeatability of this method, the THz signal of each sample was measured 3 times, then the average signal was processed to obtain the results discussed below. All measurements were carried at ambient temperature about 21°C.

3. Optical parameters and effective dielectric function calculus

From the experimental time-domain THz data of the *Pouteria sapota* samples was possible determine the complex refractive index $\widehat{n} = n + i\kappa$, where n is refractive index and k is

extinction coefficient of the material. These optical parameters can be calculated by analyzing the intensity changes and the phase delay that the THz pulse undergoes as it propagates through the sample. For this, it is necessary translates the experimentally measured THz signals, $E(t)$, into the frequency domain through the Fast Fourier Transform, obtaining a spectrum, $E(\omega)$, where $\omega = 2\pi c/\lambda$.

The spectra of the THz data when propagating in air $E_{ref}(\omega)$ and then through the sample $E_s(\omega)$, are related by Eq. (2), which represents the complex transmittance $T(\omega)$ of the sample with thickness d at normal incidence [16]. Where $A(\omega)$ is the amplitude ratio and $\phi(\omega)$ is the relative phase difference between the sample and reference spectra.

$$T(\omega) = \frac{E_s(\omega)}{E_{ref}(\omega)} = \frac{4n(\omega)}{[n(\omega)+1]^2} e^{\frac{-\alpha(\omega)d}{2}} \times e^{\frac{-i\omega[n(\omega)-1]d}{c}} = A(\omega)e^{-i\phi(\omega)}. \quad (2)$$

Considering that the thickness of each sample is comparable to or larger than the wavelength (1 THz = 300 μm), the value the refractive index is calculated by Eq. (3).

$$n(\omega) = 1 + \frac{c}{\omega d}\phi(\omega). \quad (3)$$

The absorption coefficient of the sample is found by Eq. (4).

$$\alpha(\omega) = -\frac{2}{d}\ln[A(\omega)]\frac{[n(\omega)+1]^2}{4n(\omega)}, \quad (4)$$

and the extinction coefficient is related to $\alpha(\omega)$ by Eq. (5)

$$\kappa(\omega) = \frac{\alpha(\omega)\lambda}{4\pi}. \quad (5)$$

Due to some materials exhibit strong absorption peaks at specific THz frequencies, it is possible to extract information about the structure of the sample and its compounds, once the absorption coefficient and refractive index have been calculated [27-29].

Then, after calculating the values of $n(\omega)$ and $\kappa(\omega)$, the parameters of the complex dielectric properties of each sample are calculated using Eqs. (6) and (7). Where $\varepsilon_r(\omega)$ is the dielectric constant that relate to the ability to store energy of a material, and $\varepsilon_i(\omega)$ is the dielectric loss factor that related to the electromagnetic energy into heat [16].

$$\varepsilon_r(\omega) = n(\omega)^2 - \kappa(\omega)^2, \quad (6)$$

$$\varepsilon_i(\omega) = 2n(\omega)\kappa(\omega). \quad (7)$$

Finally, these parameters are related to the complex dielectric function, $\epsilon(\omega)$, through Eq. (8). It is important to mention that all materials have a unique dielectric property that depends on the excitation frequency range (ω).

$$\varepsilon(\omega) = \varepsilon_r(\omega) - i\varepsilon_i(\omega). \quad (8)$$

In this work, *Pouteria sapota* slab is considered as a complex-structured mixture of different compounds. Therefore, the complex dielectric function $\varepsilon(\omega)$, calculated from $T(\omega)$, is called as an effective dielectric function ε_{eff}.

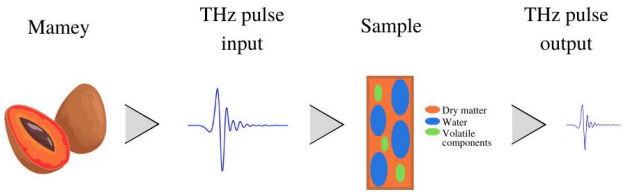

FIGURE 1. Illustration of cross section of *Pouteria sapota* slab formed by dry matter, water, and VC.

3.1. Modelling of the effective dielectric function using the Landau-Lifshitz-Looyenga model

The EDF calculated in Eq. (8) describes the sum of the contribution of all the components contained in the *Pouteria Sapota* sample. To determine the dielectric function and the volume fraction of each compound in the sample of each of them, it is necessary to apply the effective medium theory. Our proposal establishes the presence of other substances in organic matter that contribute to its dielectric (and organoleptic) properties and that have not been taken into account in the literature. Hence, we consider that *Pouteria sapota* slab is not only constituted by solid/dry matter and water, but also has volatile components, as show in Fig. 1. In the case of this fruit that has a high-water content, THz-TDS spectroscopy is useful to detect the water content in dry and wet samples.

There are many effective media models to analytically describe the optical and dielectric properties of a mixed material in the THz range. Some of them consider a specific characteristic of each material component. For instance, Clausius-Mossotti model assumes a uniform molecular electric field in the material; on the other side the Maxwell-Garnet and Bruggeman models consider that the inclusions have a spherical geometry, but this last model has the advantage that it also considers a different electric field for each molecule within the material. Unlike the previous ones, the Landau-Lifshitz-Looyenga model defines a material as a combination of dielectric function of its components and assumes that shapes of the particles are arbitrary [28,30]. Therefore, in this work only the LLL model was applied since the geometry of each component of the *Pouteria Sapota* is unknown.

Our analysis establishes that the calculated EDF ε_{eff} is the result of the combination of dry matter, water, and volatile components, and is defined by Eq. (9),

$$(\epsilon_{eff})^{1/3} = a_d\sqrt[3]{\varepsilon_d} + a_w\sqrt[3]{\varepsilon_w} + a_{vc}\sqrt[3]{\varepsilon_{vc}}, \quad (9)$$

where $\epsilon_{(d/w/vc)}$ and $a_{(d/w/vc)}$ are the dielectric functions and the volumetric fractions of the dry matter, water, and volatile components, respectively. Note that $a_w + a_d + a_{vc} = 1$.

First, to know the dielectric function of the dry matter, the $\varepsilon_{eff_{dry}}$ data of the totally dehydrated sample were used.

For this case, the EDF is reduced as shown in Eq. (10), assuming that there is no water content or volatile components ($a_w = 0$ and $a_{vc} = 0$) in the slab, after the dehydration process. This confirms that the ϵ_d is equal to the calculated $\varepsilon_{eff_{dry}}$. Therefore, by fitting the real and imaginary part of the data of ε_{eff_dry} to a second order polynomial, a mathematical representation of ϵ_d was obtained. This algorithm was coded in the Matlab© software (version R-2020a).

$$(\varepsilon_{eff})^{1/3} = \sqrt[3]{\varepsilon_d}. \tag{10}$$

The water dielectric function, ε_w, was obtained from a dual Debye model from the 0.2 THz to 0.9 THz range [31]. Finally, the dielectric function of the volatile components, ε_{vc}, was found from Eq. (9) using the EDF of the wet sample ($\varepsilon_{eff_{wet}}$), as show Eq. (11).

$$\sqrt[3]{\varepsilon_{vc}} = [(\varepsilon_{eff_{wet}})^{1/3} - a_d \sqrt[3]{\varepsilon_d} - a_w \sqrt[3]{\varepsilon_w}]/a_{vc}. \tag{11}$$

The value of a_w was obtained by the gravimetric method. Through an iterative process, an initial value for a_d was substituted into Eq. (11) until the theoretical function converged to the calculated dielectric function of volatile components. It was assumed that $a_{vc} = 1 - a_d - a_w$.

4. Results and discussions

4.1. Optical parameters and effective dielectric function of the samples

The average of the measured THz data and the optical parameters of the wet ($WC = 40.59$ %, 20.16 % and 15.53 %) and dry ($WC_{dry} = 0$ %) *Pouteria sapota* slabs are shown in Fig. 2. The time-domain THz data transmitted by the samples and the air are illustrated in Fig. 2a). The air signal (green line) corresponds to the reference signal, without sample. Keeping in mind that the peak-to-peak amplitude of the air signal is 100 %, an organic material is expected to reduce this value depending on the content of water and other chemical compounds. This agrees with the amplitude value of the sample with higher WC and the dry sample, which attenuate the reference signal up to 43.9 % and 6.5 %, respectively. This indicates that the amplitude of the THz signal transmission is directly related to water content in a sample. It can also be noticed a time delay in the phase of the THz signals from the reference signal which is attributed to the refractive index and thicknesses of the sample. Considering the three different signals measured in each sample, the mean absolute error (MAE) and the standard deviation (SD) were calculated for each case. This statistical analysis shows that the maximum value of MAE was 0.002 for the dry sample with a SD of 0.002. The MAE and SD values decrease as the water content in the sample increases. For example, for the most humid sample, MAE = 3.977e-04 and SD = 5.507e-04 were obtained. This is consistent since the THz signal for a wet sample is attenuated by the presence of water molecules; then the experimental error is reduced as it is a signal of small amplitude. This result indicates that the dispersion of the points in the different measurements is almost negligible. On average, the relative error in measurements was no more than 2.067%. Some factors that possibly contribute to this percentage error are temperature variation during measurements, water content, and non-homogeneous thickness of the sample.

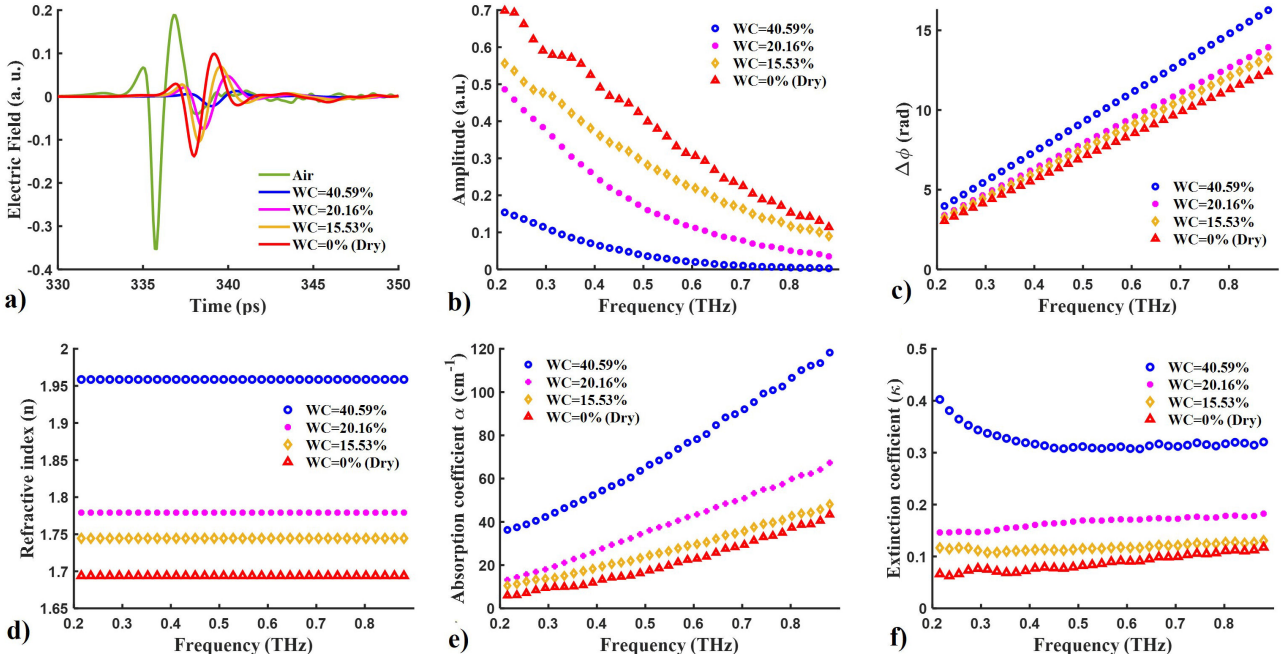

FIGURE 2. THz signals measured in the time domain a), and the amplitude b) and phase difference c) spectra in the frequency domain of the transmittance of the *Pouteria sapota* samples with water content of 40.59% (○), 20.16% (●), 15.53% (◊) and 0% (△). Calculated optical constants: refractive index d), absorption e) and extinction f) coeficients of each slab.

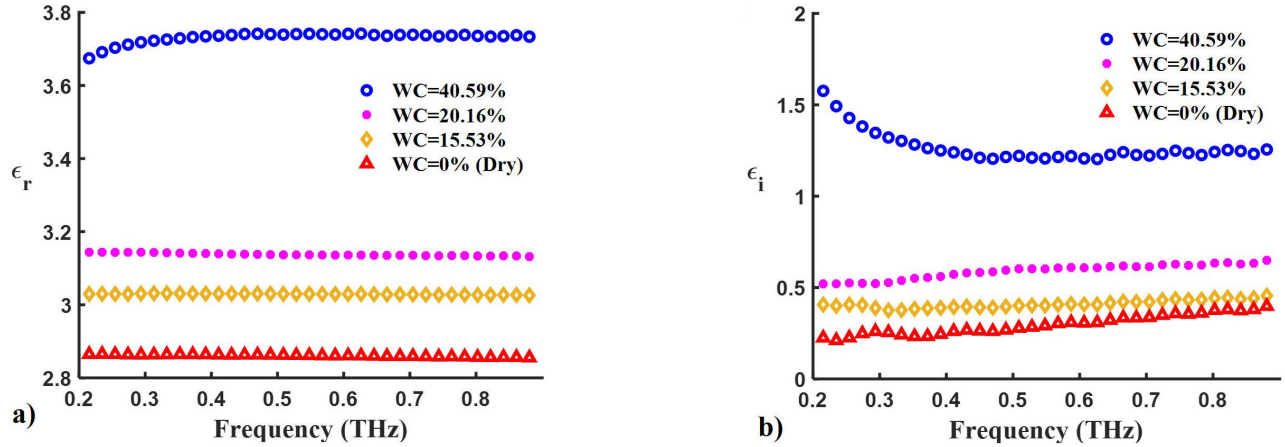

FIGURE 3. Real a) and imaginary b) parts of the calculated effective dielectric function of samples with water content of 40.59% (○), 20.16% (●), 15.53% (◊) and 0% (△).

After calculating the Fast Fourier Transform of each average spectrum to convert from the time to frequency domain spectrum, the amplitude and the phase difference of the complex transmittance of the samples were calculated in the frequency ranges from 0.2 to 0.9 THz. As shown Fig. 2b), the amplitude value decreases as the water content in the sample increases. Note that the amplitude of the dry sample spectrum decays to zero starting at 0.8 THz. On the other hand, the phase difference [Fig. 2c)] increases as a function of the WC in the sample. Regarding the optical parameters calculated by Eqs. (3) to (5), the real and the imaginary part part of the complex refractive index are shown in Fig. 2d) and 2f), respectively. The average refractive index [Fig. 2d)] for the dry sample is around $n = 1.694$, which is lower than that of the wet samples. For the slabs with WC of 40.59%, 20.16% and 15.53%, the n values are 1.959, 1.779 and 1.744, respectively. The absorption coefficient [Fig. 2e)] of the wet samples increases rapidly compared to the dry one. This behavior confirms that water molecules are more sensitive to the higher terahertz frequency. The value of extinction coefficient [Fig. 2f)] is related to the absorption of the light. As a result, the κ value for the dry sample is expected to be lower than that for the wet samples. According to the absolute and relative error found in the THZ electric field measurements, the amplitude and phase values are not significantly affected. Consequently, the calculation of the complex refractive index parameters is not affected by possible measurement errors.

The dielectric properties, ε_r and ε_i, corresponding to the effective dielectric function ε_{eff} of the samples were calculated by Eq. (8). Figure 3 shows the calculated EDFs of the samples depending on the frequency. The dielectric constant ε_r, that indicates the ability to store energy, for the wet samples with WC of 40.59%, 20.16%, and 15.53% corresponds on average to 3.729, 3.138 and 3.029, respectively. This parameter is lower for dry sample with a value of 2.861. On the other hand, the imaginary part of ε that corresponds to the dielectric loss factor ε_i is around to 1.277, 0.588 and 0.4120 for the wet samples. The dried sample has a loss factor of 0.298. Note that the contribution of liquid compounds increases the value of ε.

4.2. Theoretical dielectric functions of the *Pouteria sapota* compounds

The dielectric functions and their volumetric fractions of dry matter, water and volatile components contained in the pulp of *Pouteria sapota* were determined using the LLL model Eq. (9). Table I summarizes the mathematical representations found to approximate the dielectric function to a second order polynomial of the dry matter and the contribution of volatile components. For each case, the real ε_r and imaginary ε_i part of its theoretical dielectric function is shown, where f represent the frequency in THz. Observe that the absolute error is very small and the correlation coefficient R^2 of the fit is close to 1. This indicates that the theoretically found dielectric function can faithfully reproduce the dielectric properties of a dry pulp or with a certain percentage of water content at any frequency. The values of a_d, a_w and a_{vc} were iteratively changed until the difference between the theoretical and experimental data was minimized. The dry matter dielectric function calculated by Eq. (10) is shown in the second row of Table I. On the other hand, the dielectric functions corresponding to the contribution of volatile components for the 3 wet samples were determined by Eq. (11). The average function that was fitted to a second-degree polynomial is shown in the third row of Table I. The values of the volumetric fractions for each wet sample were: $a_d = 0.35, a_w = 0.35$ and $a_{vc} = 0.30$ for $WC = 40.59\%$, $a_d = 0.7$, $a_w = 0.125$ and $a_{vc} = 0.175$ for $WC = 20.16\%$, and $a_d = 0.85$, $a_w = 0.05$ and $a_{vc} = 0.1$ for $WC = 15.53\%$. For dry sample these values were $a_d = 1, a_w = 0$ and $a_{vc} = 0$. Considering that this fruit has a high water content, around 85% of its weight, it is expected that the volumetric fraction of dry matter is less than the sum of water and volatile components. The theoretical approximation to the calculated data presents an absolute error almost negligible, and the R^2 value is near 1.

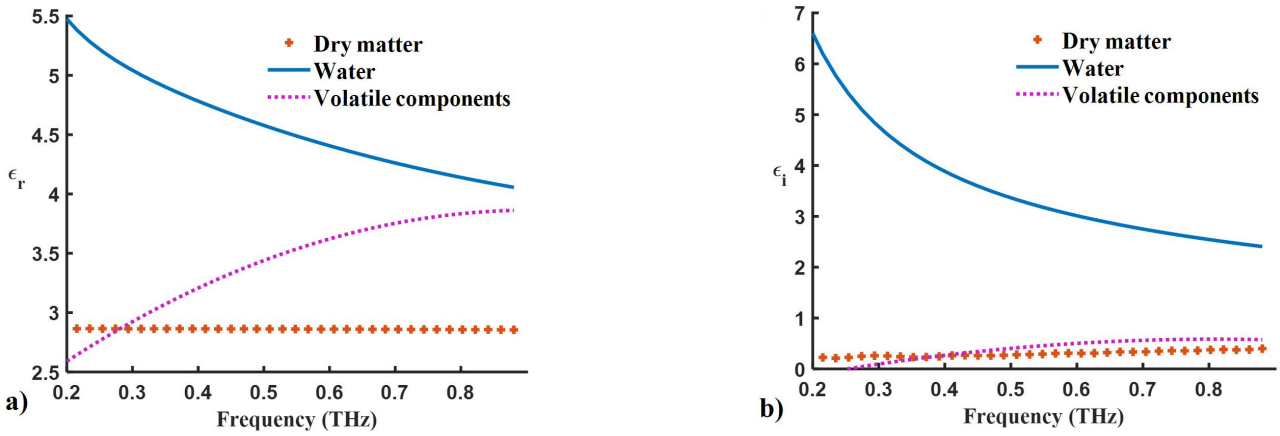

FIGURE 4. Theoretical dielectric functions of the dry matter (*), water (line) and volatile components (dot) contained in a wet sample of *Pouteria sapota*: a) ε_r and b) ε_i.

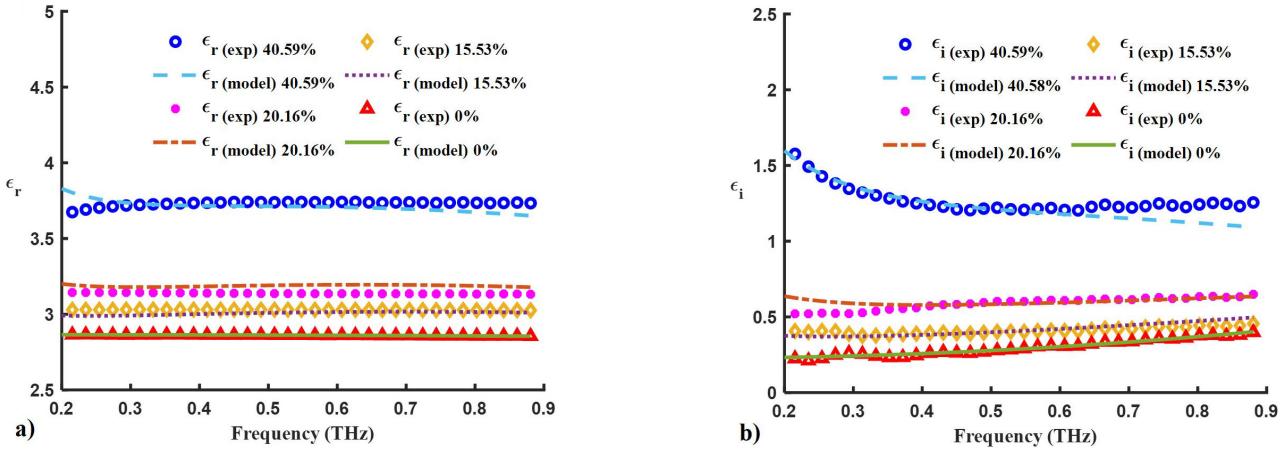

FIGURE 5. Comparison of the experimental data (represented by symbols) with the theoretical model curves (represented by dotted and solid lines) of the EDF for samples with water content of 40.59%, 20.16%, 15.53% and 0% obtained by the LLL model.

TABLE I. Theoretical dielectric function of dry matter and volatile components contained in *Pouteria sapota* slabs from 0.2 to 0.9 THz.

Compound	Theoretical dielectric function (ε)	MAE	R^2
Dry matter	$\varepsilon_{rd} = -1.7973e-26f^2 + 6.239e-15f + 2.864$	$2.467e-16$	0.964
	$\varepsilon_{id} = 2.564e-25f^2 - 2.840e-14f + 0.228$	$4.703e-17$	0.946
Volatile components	$\varepsilon_{rvc} = -2.530e-24f^2 + 4.603e-12f + 1.771$	$1.974e-16$	0.991
	$\varepsilon_{ivc} = -1.886e-24f^2 + 3.053e-12f - 0.651$	$3.354e-16$	0.950

Figure 4 shows the theoretical complex dielectric functions of the dry matter, water and volatile components contained in a wet sample of *Pouteria sapota*. The value of ε_{rd} [Fig. 4a)] is almost constant around 2.861 for the dry matter, while for the volatile components it increases from 2.575 to 3.862. This means that volatile components have a greater capacity to store electromagnetic energy than dry matter. On the other hand, Fig. 4b) illustrates the imaginary part of the dielectric function ε_i of each compound, which is usually less than ε_r. Note that the values of the dry matter and volatile components are small, no more than 0.584. This parameter represents the dielectric loss factor that is related to the energy loss when the wave passes through a *Pouteria sapota* sample and is normally converted into heat. Consequently, the water molecules and the volatile components contained in wet samples will heat up faster than dry matter from the 0.5 THz frequency.

Now, the mathematical representation of the dielectric function of each *Pouteria sapota* compound in the selected THz range is known. To determine the precision of each function, the theoretical EDFs of the samples were found and compared with the calculated one. All graphs can be seen in Fig. 5. The approximation of the dielectric functions corresponding to the wet samples present a root mean square

error (RMSE) no greater than 0.02 and with a minimum of $1.9120e-07$. It can be observed that the effective dielectric function agrees reasonably well with the theoretical curves when considering that *Pouteria sapota* sample is contained by dry matter, water and volatile components.

The application of THz-TDS for the study of the dielectric properties of *Pouteria sapota* confirms the utility of this technique as a potential tool that provides meaningful information about its mixed constituents in the THz frequency region.

Conclusion

The analysis of the interaction of the THz waves with a *Pouteria sapota* slab allowed to determine its optical parameters such as the complex refractive index and the absorption coefficient, as well as its dielectric properties in the range of 0.2 to 0.9 THz. Applying a model of the effective medium theory, such as the LLL model, the dielectric function of each constituent of the sample was approximated. For this theoretical analysis, it was considered that *Pouteria sapota* pulp is composed not only of water content and dry matter, but also includes the contribution of volatile components sensitive to temperature that can be extracted during the dehydration process. This consideration allowed to obtain a better adjustment between the experimental and theoretical data. Finally, the analysis of the behavior of this fruit in THz range is also useful to develop new drying technologies, having a place in applications in the agriculture and food processing sector for the evaluation of quality and safety in food processing. The methodology proposed here can be implemented as an in-situ and ex-situ quality control method for other fruits and vegetables in the agri-food industry.

Acknowledgements

We would like to thank Dr. R. Carriles for the support in the measurements of THz spectra. We also would like to thank S. Toledo for the help in the design of some figure. G. L. M. thanks to National Council of Humanities, Sciences and Technologies (CONAHCYT) for the postdoctoral fellowship.

1. I. Alia-Tejacal *et al.*, Postharvest physiology and technology of sapote mamey fruit (Pouteria sapota (Jacq.) H.E. Moore & Stearn), *Postharvest Biol. Technol.* **45** (2007) 285, https://doi.org/10.1016/j.postharvbio.2006.12.024.
2. E. Murillo *et al.*, Native carotenoids composition of some tropical fruits, *Food Chem.* **140** (2013) 825, https://doi.org/10.1016/j.foodchem.2012.11.014.
3. E. Yahia and F. Guttierrez-Orozco, 21 - Mamey sapote (Pouteria sapota Jacq. H. E. Moore & Stearn), In E. M. Yahia, ed., Postharvest Biology and Technology of Tropical and Subtropical Fruits, Woodhead Publishing Series in Food Science, Technology and Nutrition, pp. 482-493e (Woodhead Publishing, 2011), https://doi.org/10.1533/9780857092885.482.
4. N. Ortiz-Rodríguez *et al.*, Solar drying Technologies: A review and future research directions with a focus on agroindustrial applications in medium and large scale, *App. Therm. Eng.* **215** (2022) 118993, https://doi.org/10.1016/j.applthermaleng.2022.118993.
5. V. R. Sagar and P. S. Kumar, Recent advances in drying and dehydration of fruits and vegetables: a review, *J. Food Sci. and Technol.* **47** (2010) 15, https://doi.org/10.1007/s13197-010-0010-8.
6. C. Rodríguez *et al.*, Analysis of the Volatile Components of Pouteria sapota (Sapote Mamey) Fruit by HS-SPME-GC-MS, *Nat. Prod. Commun.* **13** (2018) 1027, https://doi.org/10.1177/1934578X1801300826.
7. G. López-Morales *et al.*, Detection of moisture ratio and carotenoid compounds in mamey (Pouteria sapota) fruit during dehydration process using spectroscopic techniques, *J. Food Sci. Technol.* **60** (2023) 1952, https://doi.org/10.1007/s13197-023-05728-w.
8. J. Alander *et al.*, A Review of Optical Nondestructive Visual and Near-Infrared Methods for Food Quality and Safety, *Int. J. Spectrosc.* **2013** (2013), https://doi.org/10.1155/2013/341402.
9. K. B. Walsh *et al.*, Visible-NIR 'point' spectroscopy in postharvest fruit and vegetable assessment: The science behind three decades of commercial use, *Postharvest Biol. Technol.* **168** (2020) 111246, https://doi.org/10.1016/j.postharvbio.2020.111246.
10. S. Khushbu *et al.*, Recent Advances in Terahertz Time-Domain Spectroscopy and Imaging Techniques for Automation in Agriculture and Food Sector, Food Anal. *Methods* **15** (2022) 498, https://doi.org/10.1007/s12161-021-02132-y.
11. S. Zappia, L. Crocco, and I. Catapano, THz Imaging for Food Inspections: A Technology Review and Future Trends, In B. You and J.-Y. Lu, eds., Terahertz Technology, chap. 5 (IntechOpen, Rijeka, 2021), https://doi.org/10.5772/intechopen.97615.
12. L. Zhang, M. Zhang, and A. S. Mujumdar, Terahertz Spectroscopy: A Powerful Technique for Food Drying Research, *Food Rev. Int.* **39** (2021) 1733, https://doi.org/10.1080/87559129.2021.1936004.
13. H. Arteaga, N. León-Roque, and J. Oblitas, The frequency range in THz spectroscopy and its relationship to the water content in food: A first approach, *Sci. Agropecu.* **12** (2021) 625, https://doi.org/10.17268/sci.agropecu.2021.066.
14. H-Domínguez *et al.*, First Principles for Evaluation of the Moisture Content in Mango Slice by Tera-Hertz Pulses, In 2018 15th International Conference on Electrical Engineering, Computing Science and Automatic Control (CCE) (2018)

pp. 1-4, https://doi.org/10.1109/ICEEE.2018.8533906.

15. G.-H. Oh *et al.*, In-situ monitoring of moisture diffusion process for wood with terahertz time-domain spectroscopy, *Opt. Lasers Eng.* **128** (2020) 106036, https://doi.org/10.1016/j.optlaseng.2020.106036.
16. H. J. Shin *et al.*, Dielectric traces of food materials in the terahertz region, *Infrared Phys. & Technol*. **92** (2018) 128, https://doi.org/10.1016/j.infrared.2018.05.022.
17. M. Sosa-Morales *et al.*, Dielectric properties of foods: Reported data in the 21st Century and their potential applications, *LWT - Food Sci. and Technol.* **43** (2010) 1169, https://doi.org/10.1016/j.lwt.2010.03.017.
18. E. Castro-Camus *et al.*, Industrial Applications of Terahertz Waves, In H.-J. Song and T. Nagatsuma, eds., Handbook of Terahertz Technologies: Devices and Applications (1st ed.), chap. 16 (CRC Press, New York, 2015), https://doi.org/10.1201/b18381.
19. T. K. Kataria *et al.*, Dielectric properties of guava, mamey sapote, prickly pears, and Nopal in the microwave range, *Int. J. Food Prop.* **20** (2017) 2944, https://doi.org/10.1080/10942912.2016.1261154.
20. K. Solyom *et al.*, Effect of temperature and moisture contents on dielectric properties at 2.45 GHz of fruit and vegetable processing by-products, *RSC Adv.* **10** (2020) 16783, https://doi.org/10.1039/C9RA10639A.
21. Z. Zhu and W. Guo, Frequency, moisture content, and temperature dependent dielectric properties of potato starch related to drying with radio-frequency/microwave energy, *Sci. Rep.* **7** (2017) 9311, https://doi.org/10.1038/s41598-017-09197-y.
22. Y. Ueno *et al.*, Quantitative measurements of amino acids by terahertz time-domain transmission spectroscopy, *Anal. Chem.* **78** (2006) 5424, https://doi.org/10.1021/ac060520y.
23. P. Parasoglou *et al.*, Quantitative water content measurements in food wafers using terahertz radiation, *Terahertz Sci. Technol.* **3** (2010) 176, https://doi.org/10.11906/TST.172-182.2010.12.17.
24. Y. Jiang, H. Ge, and Y. Zhang, Quantitative analysis of wheat maltose by combined terahertz spectroscopy and imaging based on Boosting ensemble learning, *Food Chem.* **307** (2020) 125533, https://doi.org/10.1016/j.foodchem.2019.125533.
25. K. Shiraga *et al.*, Quantitative characterization of hydration state and destructuring effect of monosaccharides and disaccharides on water hydrogen bond network, *Carbohydr. Res.* **406** (2015) 46, https://doi.org/10.1016/j.carres.2015.01.002.
26. S. Nakajima *et al.*, Quantification of starch content in germinating mung bean seedlings by terahertz spectroscopy, *Food Chem.* **294** (2019) 203, https://doi.org/10.1016/j.foodchem.2019.05.065.
27. R. Gente *et al.*, Determination of leaf water content from terahertz time-domain spectroscopic data, J. Infrared Milli. *Terahz Waves* **34** (2013) 316, https://doi.org/10.1007/s10762-013-9972-8.
28. G. Hernandez-Cardoso, A. K. Singh, and E. Castro-Camus, Empirical comparison between effective medium theory models for the dielectric response of biological tissue at terahertz frequencies, *Appl. Opt.* **59** (2020) D6, https://doi.org/10.1364/AO.382383.
29. J. F. Federici, Review of moisture and liquid detection and mapping using terahertz imaging, *J. Infrared Milli. Terahz Waves* **33** (2012) 97, https://doi.org/10.1007/s10762-011-9865-7.
30. M.Scheller, C. Jansen, and M. Koch, Applications of Effective Medium Theories in the Terahertz Regime, In K. Y. Kim, ed., Recent Optical and Photonic Technologies, chap. 12 (IntechOpen, Rijeka, 2010), https://doi.org/10.5772/6915.
31. H. Liebe, G. Hufford, and T. Manabe, A model for the complex permittivity of water at frequencies below 1 THz, *Int. J. Infrared Milli Waves* **12** (1991) 659, https://doi.org/10.1007/BF01008897.